NACA RM E51G14

NACA

RESEARCH MEMORANDUM

EXPERIMENTAL INVESTIGATION OF AN 0.8 HUB-TIP RADIUS-RATIO, NONTWISTED-ROTOR-BLADE TURBINE

By David H. Silvern and William R. Slivka

Lewis Flight Propulsion Laboratory
Cleveland, Ohio

NATIONAL ADVISORY COMMITTEE
FOR AERONAUTICS

WASHINGTON
December 12, 1951

NATIONAL ADVISORY COMMITTEE FOR AERONAUTICS

RESEARCH MEMORANDUM

EXPERIMENTAL INVESTIGATION OF AN 0.8 HUB-TIP RADIUS-RATIO, NONTWISTED-ROTOR-BLADE TURBINE

By David H. Silvern and William R. Slivka

SUMMARY

An experimental investigation of an 0.8 hub-tip radius-ratio, nontwisted-rotor-blade turbine designed for a stagnation-pressure ratio of 2.5 and an equivalent mean blade speed of 643 feet per second was made in a cold-air turbine with (a) twisted stator blades designed to maintain zero rotor-inlet incidence angles at all radii and (b) nontwisted stator blades designed to maintain zero rotor-inlet incidence angles at the mean radius only.

Turbine efficiencies of approximately 0.85 at the design point were obtained with a nontwisted-rotor-blade turbine with a hub-tip radius ratio of 0.80. The turbine with the twisted stator blades gave higher efficiencies at the design point (of approximately 1.5 percentage points) than the turbine with the nontwisted stator blades.

INTRODUCTION

The application of internal turbine-rotor-blade cooling to aircraft gas-turbine engines introduces certain complications to blade fabrication. In order to simplify fabrication of blades both for internal cooling and for turbines for expendable engines, where economy of manufacture is of utmost importance, simple blade forms are desirable. One of the simplest rotor blade forms is one of uniform camber and zero twist along the blade height. Analytical investigations of this type turbine-rotor blade are reported in references 1 and 2. Reference 1 presents an analysis of the flow conditions in a turbine stage consisting of nontwisted rotor blades in combination with nontwisted stator blades. The results of this study indicate that rotor-blade incidence angles are encountered, but that these angles are reduced by use of high hub-tip radius ratios. An analysis of the flow conditions in a turbine stage consisting of nontwisted rotor blades in combination with twisted stator blades designed to maintain zero rotor-entrance incidence angles is presented in reference 2. This analysis indicates that the aerodynamic characteristics of these turbines are approximately those of free-vortex turbines intended for similar applications.

In order to evaluate the aerodynamic characteristics of nontwisted rotor-blade turbines, an experimental investigation was conducted at the NACA Lewis laboratory on an 0.80 hub-tip radius-ratio, nontwisted-rotor-blade turbine tested successively in combination with (a) twisted stator blades designed to maintain zero rotor-inlet incidence angles at all radii and (b) nontwisted stator blades designed to maintain zero rotor-inlet incidence angles at the mean radius only. These investigations were conducted on a single-stage cold-air turbine having a tip diameter of 14.72 inches with inlet conditions of atmospheric pressure and a temperature of 710° R. Over-all performance data were obtained over a range of equivalent, mean blade speeds from 350 to 800 feet per second and stagnation pressure ratios from 1.75 to 4.0.

SYMBOLS

The following symbols are used in this report:

A	annulus area, square feet
g	acceleration due to gravity, feet per second per second
h	enthalpy, Btu per pound
$\Delta h'$	turbine-stagnation enthalpy drop, Btu per pound
M	Mach number based on speed of sound at static state
p	pressure, pounds per square inch
R	gas constant, foot-pounds per pound per °F
r	radius, inches
T	temperature, °R
U	blade speed, feet per second
V	absolute velocity, feet per second
W	relative velocity, feet per second
w	gas weight flow, pounds per second
α	angle of absolute velocity from tangential direction, degrees
β	angle of relative velocity from tangential direction, degrees
$(\beta_d-\beta)_2$	rotor incidence angle, degrees

γ	ratio of specific heats
δ	ratio of inlet total pressure to NACA standard sea-level pressure
η_t	turbine-brake internal efficiency based on stagnation conditions
θ	ratio of inlet total temperature to NACA standard sea-level temperature

Subscripts:

1	turbine inlet
2	stator outlet, rotor inlet
3	rotor outlet
d	design
m	mean
s	isentropic
u	tangential
x	axial

Superscript:

'	stagnation state

TURBINE DESIGN

General Specifications

The turbine having twisted stator blades was designed according to the following specifications:

Equivalent mean blade speed, $U_m/\sqrt{\theta_1}$, ft/sec	643
Stagnation-pressure ratio at mean radius, $p_{m,1}'/p_{m,3}'$	2.50
Exit whirl at rotor outlet mean radius, $V_{u,3}$, ft/sec	0
Equivalent weight flow, $w\sqrt{\theta_1}/\delta_1$, lb/sec	5.67
Turbine hub-tip radius ratio at midaxial chord position of rotor blade	0.80
Turbine outside diameter at midaxial chord position of rotor blade, in.	14.72

The following assumptions were made in the design:

(1) The stagnation pressure and the stagnation temperature are uniform over the blade height at the inlet to the stator and rotor.

(2) The expansion in the turbine is adiabatic.

(3) The average velocity coefficient (ratio of actual to ideal velocity) for the stator is 0.985.

(4) The ratio of the effective annulus area to the actual annulus area between the stator outlet and rotor inlet is 0.980.

(5) The flow losses in the rotor reduce the kinetic energy by 3 Btu per pound. (A design brake internal efficiency of 0.89 results.)

(6) Simplified radial equilibrium exists at the stator and the rotor outlets.

(7) No diffusion of stator and rotor blade wakes occurs at stations 2 and 3.

By using these design requirements and assumptions, the mean radius velocity diagrams at the stator and rotor outlets were calculated. The velocity diagrams for the hub and tip radii, when zero rotor-inlet incidence angles $(\beta_d-\beta)_2$ were maintained (twisted stator), were obtained in accordance with the methods described in reference 2. These velocity diagrams are presented in figure 1 for the hub, mean, and tip radii. The relative rotor-inlet Mach number at the hub is equal to 0.703 and a small pressure drop (reaction, which is defined by $\frac{W_3^2-W_2^2}{W_2^2}$, equal to 0.19) exists across the rotor hub.

When the stator-outlet angle was held constant along the radius, the rotor incidence angles for the nontwisted rotor blade were calculated in accordance with the methods presented in reference 1. These results are presented in figure 2 where rotor-inlet incidence angle is plotted against radius ratio. The incidence angle varies from 0° at the mean radius to 8° and -13° at the hub and tip, respectively.

Blade Design

Stator blades. - The outlet angle and the cross section of the nontwisted stator blades were made to conform to those of the mean radius of the twisted stator blades. The mean-radius cross section of

a stator blade is shown in figure 3. The mean-radius profile has a 1/16-inch constant thickness distribution and was designed in the following manner: The mean line had a short, straight axial section AB (fig. 3(a)), the mean line from B to C was made up of three arbitrary circular arcs of increasing radius, and the remainder of the line from C to D was straight and tangent to the curved section at point C. The sections at the other radii were constructed in a similar manner for the case where zero rotor-inlet incidence angles are maintained along the radius. The stator-blade assembly consisted of 36 sheet-metal blades welded to two concentric, cylindrical rings. The fillets thus formed at the roots and at the tips of the blades were hand-finished to provide smooth flow passages.

Rotor blades. - The rotor blades were investigated with both the twisted and nontwisted stator blades. The mean section of the rotor blade, which is shown in figure 3(b), was designed for zero angle of incidence; that is, the air angle β is equal to the blade camber angle and the same cross section was maintained at all radii. The blade profile was constructed in the following manner: An involute of a circle was arbitrarily selected as the part of the suction surface between points A and B (fig. 3(b)). The involute of a circle provides the suction surface with a gradually increasing radius of curvature. From the downstream end of the involute (point A, fig. 3(b)), the contour was faired to meet the straight line that extends from E to the trailing-edge circle. Upstream of the involute, the suction surface was faired from point B to the leading-edge circle.

The pressure surface (concave surface of the rotor blade) was determined by specifying a convergent channel with a smooth area variation. The turbine wheel was made up of 150 blades that were 1.47 inches long with an axial chord of 0.6 inch. The axial clearance between the stator and rotor blades was 0.18 inch. Each blade was made with an integral cap at the tip, which formed a shroud when the blades were clamped together. A cross-sectional view of the turbine-blade configuration showing mechanical details is presented in figure 4(a).

EXPERIMENTAL EQUIPMENT AND INSTRUMENTATION

Ambient air was drawn through an electrostatic precipitator that removed foreign material. In order to avoid water condensation in the turbine, the filtered air was heated by passing through a thermostatically controlled air heater. After passing through the turbine, the air was exhausted by the laboratory low-pressure exhaust system. The power output of the turbine was absorbed by a water brake that was cradle-mounted for torque measurement.

A cross section of the turbine showing the location of the instrumentation is presented in figure 4(b). Entrance stagnation pressure p_1' was indicated by four stagnation-pressure tubes 0.75 inch upstream of the stator blades; a circumferential and radial stagnation-pressure survey at the stator inlet was made to insure that these tubes indicated the average inlet stagnation pressure. The inlet stagnation temperature was measured with four stagnation-type probes that were arranged circumferentially and located at the same axial station as were the stagnation-pressure probes. The rotor-outlet static pressure was measured with 12 wall taps located 0.72 inch downstream of the rotor that were evenly spaced circumferentially, six on the inner exhaust-guide shell and six on the outer exhaust-guide shell. The outlet total temperature was measured with three stagnation-type thermocouples at the downstream end of the two exhaust-guide shells. Although the temperature variation along the radius may have prevented these thermocouples from accurately indicating an average temperature, the effect on turbine performance is small because this temperature was used only to compute rotor-outlet stagnation pressure (the method of obtaining outlet stagnation pressure is described in the section entitled "Procedure and Performance Calculations.") Thus an error of 5° R would change the computed efficiency less than 0.003.

Torque was measured with a commercial springless dynamometer scale. Air flow was measured with a submerged 7-inch flat-plate orifice upstream of the air heater. Turbine speed was indicated by a calibrated electric tachometer.

The instruments were read with the following precision:

Absolute pressure, inch of tetrabromoethene	±0.05
Temperature, $^\circ$R	±1
Orifice pressure drop, inch of water	±0.05
Torque load, pound	±0.2
Rotative speed, rpm	±13

For a stagnation-pressure ratio of 2.00 or greater, the probable error in reproducing the turbine efficiency was ±0.005.

PROCEDURE AND PERFORMANCE CALCULATIONS

Data were taken at nominal values of stagnation-pressure ratio from 1.75 to 4.0. At each of the pressure ratios, the turbine was operated at rotor equivalent mean blade speeds from 350 to 800 feet per second. For all runs, the inlet stagnation temperature was maintained between 708° and 712° R; the stator-inlet stagnation pressure varied between 26 and 29 inches of mercury, depending upon the air flow and the local barometric pressure.

The brake internal efficiency, which is based on expansion between the inlet and outlet stagnation pressures, was used to express the performance of the turbine; this efficiency is defined as

$$\eta_t = \frac{\Delta h'}{(h_1' - h_3')_s}$$

where $\Delta h'$ is determined from turbine-shaft work. The ideal drop in enthalpy $(h_1' - h_3')_s$ was computed from the chart of air properties in reference 3 by using the inlet stagnation pressure and temperature and the outlet stagnation pressure. The outlet stagnation pressure was computed by using the following formula in which all quantities are known except p_3'.

$$\frac{w\sqrt{T_3'}}{p_3 A_3} = \frac{p_3'}{p_3}\sqrt{\left(\frac{p_3}{p_3'}\right)^{\frac{2}{\gamma}} - \left(\frac{p_3}{p_3'}\right)^{\frac{\gamma+1}{\gamma}}}\left[\left(\frac{2\gamma}{\gamma-1}\right)\left(\frac{g}{R}\right)\right]^{\frac{1}{2}}$$

This method of computing the outlet stagnation pressure gives a conservative value because any energy available from the tangential component of the velocity is neglected. The weight flow of air was determined from the orifice measurements together with the data of reference 4.

All turbine-performance data were reduced to NACA standard sea-level conditions at the rotor inlet. The performance was expressed in terms of the following variables: brake internal efficiency, η_t; stagnation-pressure ratio, p_1'/p_3'; equivalent turbine-stagnation enthalpy drop, $\Delta h'/\theta_1$; ratio of equivalent mean blade speed to equivalent weight flow, $U_m \delta_1/w\theta_1$; equivalent mean blade speed, $U_m/\sqrt{\theta_1}$.

RESULTS AND DISCUSSION

The over-all performance of the nontwisted-rotor-blade turbine is presented in the form of a composite plot where the parameters of brake internal efficiency, equivalent mean blade speed, and stagnation-pressure ratio are plotted against equivalent turbine stagnation enthalpy drop as the ordinate and the ratio of equivalent mean blade speed to equivalent weight flow as the abscissa (fig. 5). A comparison of the turbine with twisted and with nontwisted stator blades is also presented on a cross plot of brake internal efficiency against equivalent mean blade speed for constant stagnation-pressure ratio (fig. 6).

The over-all performance of the turbine with the nontwisted rotor blades and the stator designed to maintain zero rotor-inlet incidence angles is shown in figure 5(a). At the design point the turbine efficiency is 0.855 and the maximum efficiency occurs at higher than design-pressure ratio and blade speed (with hub relative rotor-inlet Mach numbers of approximately 0.80).

The over-all performance of the turbine with nontwisted rotor blades and the nontwisted stator blades is shown in figure 5(b). The turbine efficiency at the design point, that is, where the flow conditions at the mean radius are the same as for the twisted-stator configuration, is 0.84. Here again, the maximum turbine efficiency occurs at higher than design pressure ratio and blade speed.

In order to compare the performance of the two turbine configurations investigated more efficiently, cross plots of the turbine efficiency for constant stagnation-pressure ratios of 2.5 (design), 3.5, and 1.75 were made. This comparison is presented in figures 6(a), 6(b), and 6(c), respectively, where brake internal efficiency is plotted against equivalent mean blade speed. At the design stagnation-pressure ratio of 2.5 (fig. 6(a)), maximum efficiency occurs at design speed (643 ft/sec) for both turbines. An improvement of 1.5 percentage points is obtained at design speed by using the twisted stator blades rather than the nontwisted stator blades. The decrease in the efficiency of the turbine with nontwisted stator blades is probably due to the rotor-inlet incidence angles shown in figure 2. The effect of incidence angle for various Mach numbers is shown in reference 5. This effect is seen to be small for the angles of attack encountered in this investigation. Similar plots for stagnation-pressure ratios of 3.50 and 1.75, respectively, are shown in figures 6(b) and 6(c). A maximum improvement of 1 percentage point at a stagnation-pressure ratio of 3.50 and an improvement of 4 percentage points at a pressure ratio of 1.75 is obtained with the use of twisted stator blades.

SUMMARY OF RESULTS

An experimental investigation of an 0.80 hub-tip radius ratio, nontwisted-rotor-blade turbine was made with: (a) twisted stator blades designed to maintain zero rotor-inlet incidence angles at all radii and (b) nontwisted stator blades designed to maintain zero rotor-inlet incidence angles at the mean radius only. The following results were obtained in a single-stage turbine having a tip diameter of 14.72 inches with inlet conditions of atmospheric pressure and a temperature of 710° R:

1. Turbine efficiencies of approximately 0.85 at the design point were obtained with a nontwisted-rotor-blade turbine with a hub-tip radius ratio of 0.80.

2. The turbine with the twisted stator blades designed to maintain zero rotor-inlet incidence angles at all radii gave higher efficiencies at the design point (approximately 1.5 percentage points) than the turbine with the nontwisted stator blades designed to maintain zero rotor-inlet incidence angles at the mean radius only.

3. At off-design point operation, the maximum improvement of the turbine efficiency with the use of twisted stator blades varied from 4 percentage points at a stagnation pressure ratio of 1.75 to 1 percentage point at a stagnation-pressure ratio of 3.50.

Lewis Flight Propulsion Laboratory
National Advisory Committee for Aeronautics
Cleveland, Ohio

REFERENCES

1. Eckert, and Korbacher: The Flow through Axial Turbine Stages of Large Radial Blade Length. NACA TM 1118, 1947.

2. Slivka, William R., and Silvern, David H.: Analytical Evaluation of Aerodynamic Characteristics of Turbines with Nontwisted Rotor Blades. NACA TN 2365, 1951.

3. Amorosi, A.: Gas Turbine Gas Charts. Res. Memo. No. 6-44 (Navships 250-330-6), Bur. Ships, Navy Dept., Dec. 1944.

4. Anon.: Fluid Meters, Their Theory and Application. A.S.M.E. Res. Pub., Pub. by Am. Soc. Mech. Eng. (New York), 4th ed., 1937.

5. Ainley, D. G.: Performance of Axial-flow Turbines. War Emergency Issue No. 41, pub. by Inst. Mech. Eng. (London). (Reprinted in U.S.A. by ASME, April 1949, pp. 230-244.)

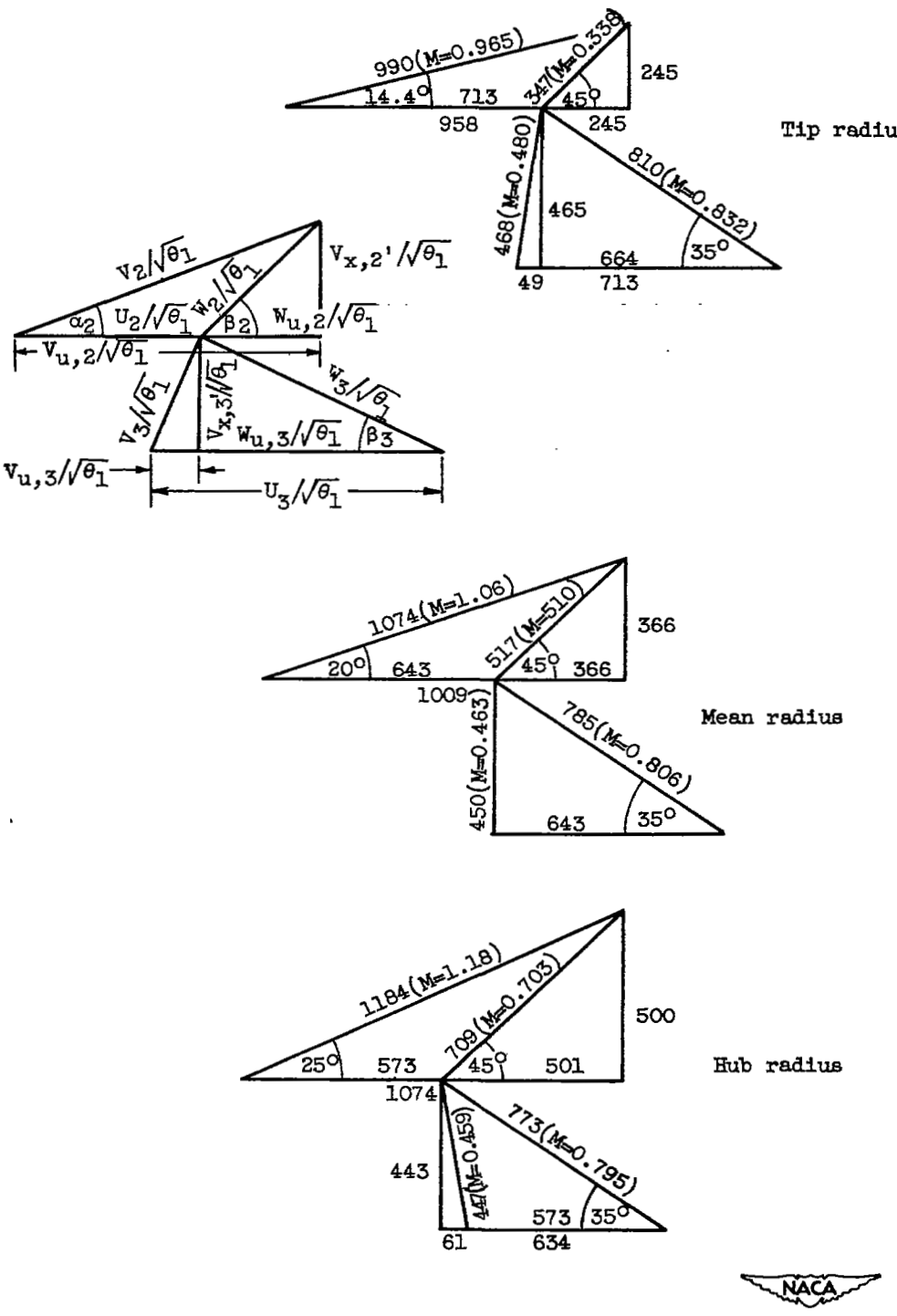

Figure 1. - Design velocity diagrams for nontwisted rotor-blade turbine with stator designed for zero incidence angles (twisted stator).

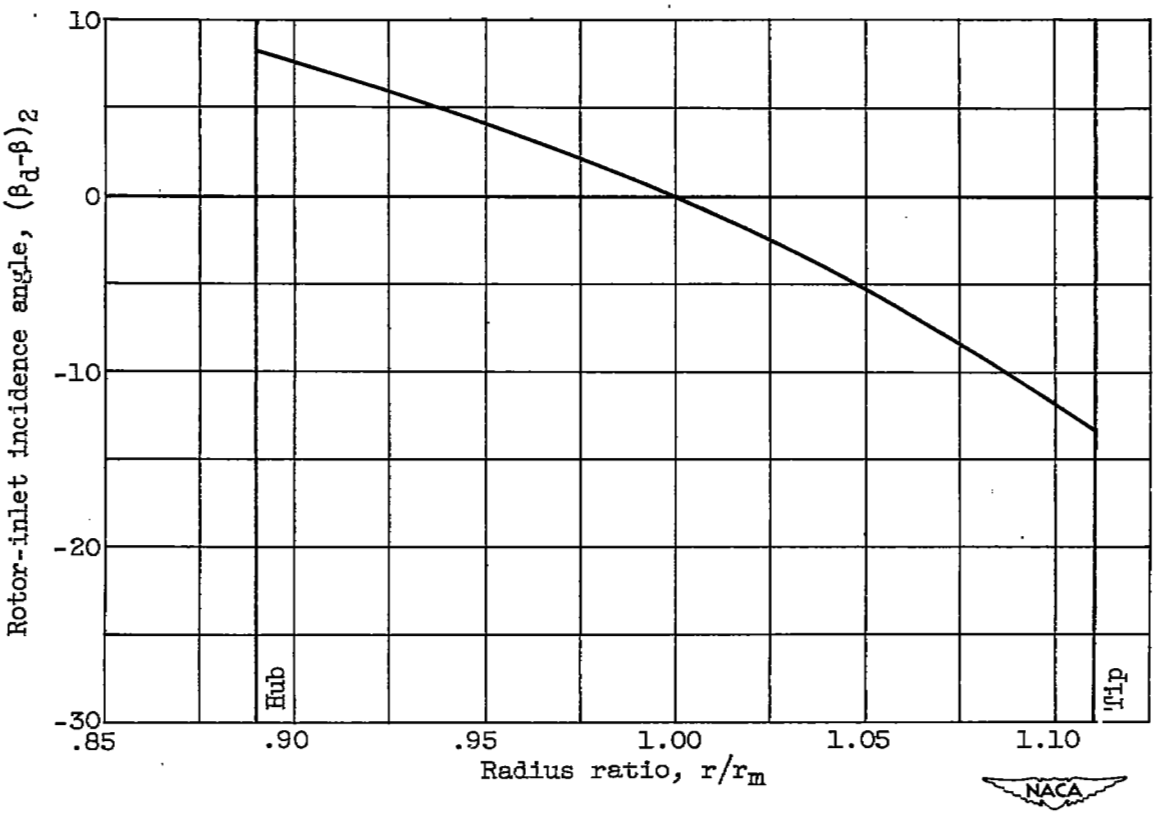

Figure 2. - Computed rotor-inlet incidence angles for nontwisted rotor when used with nontwisted stator.

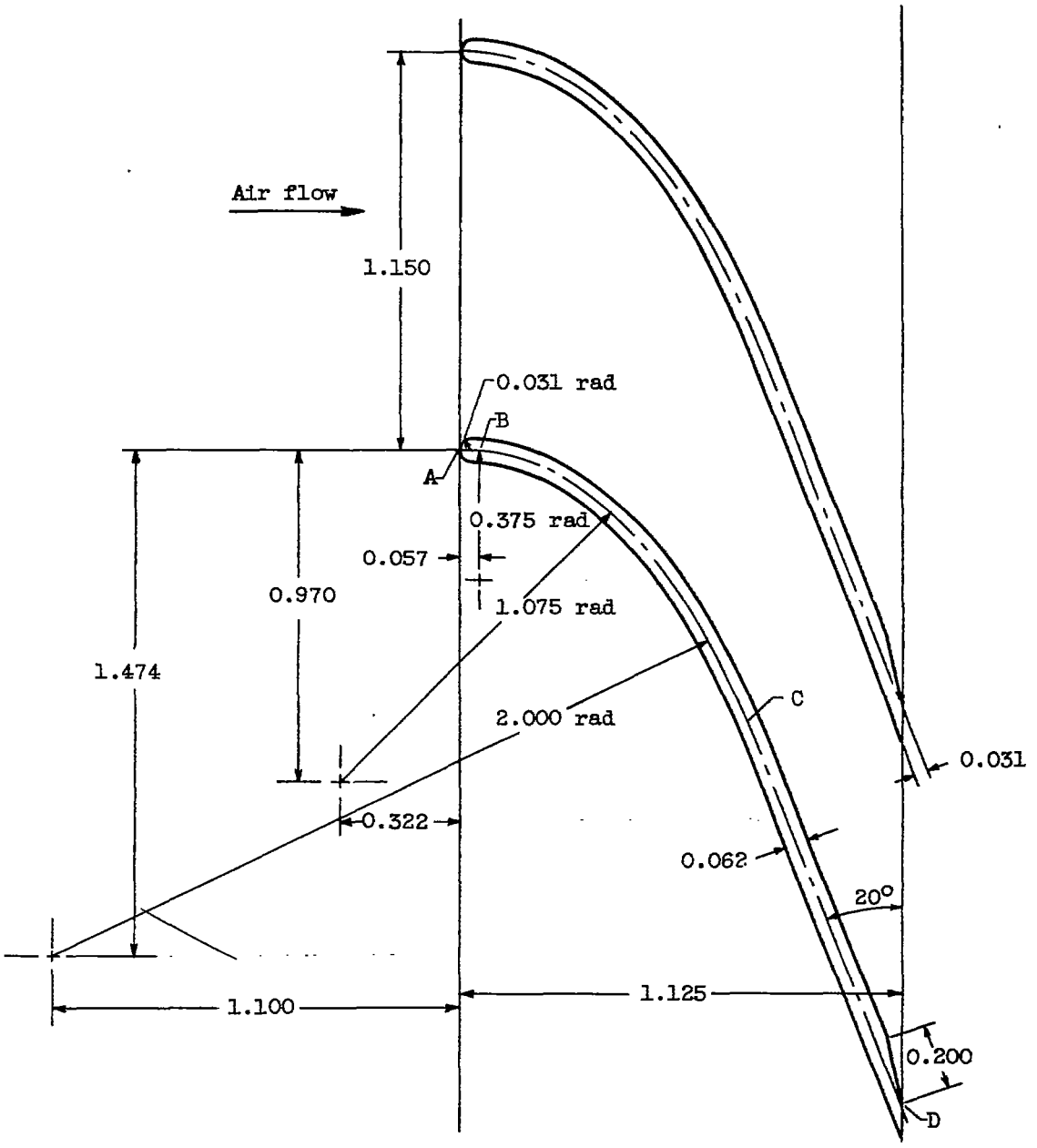

(a) Twisted and nontwisted stator blades.

Figure 3. - Mean-section profiles of blades. (All dimensions in inches.)

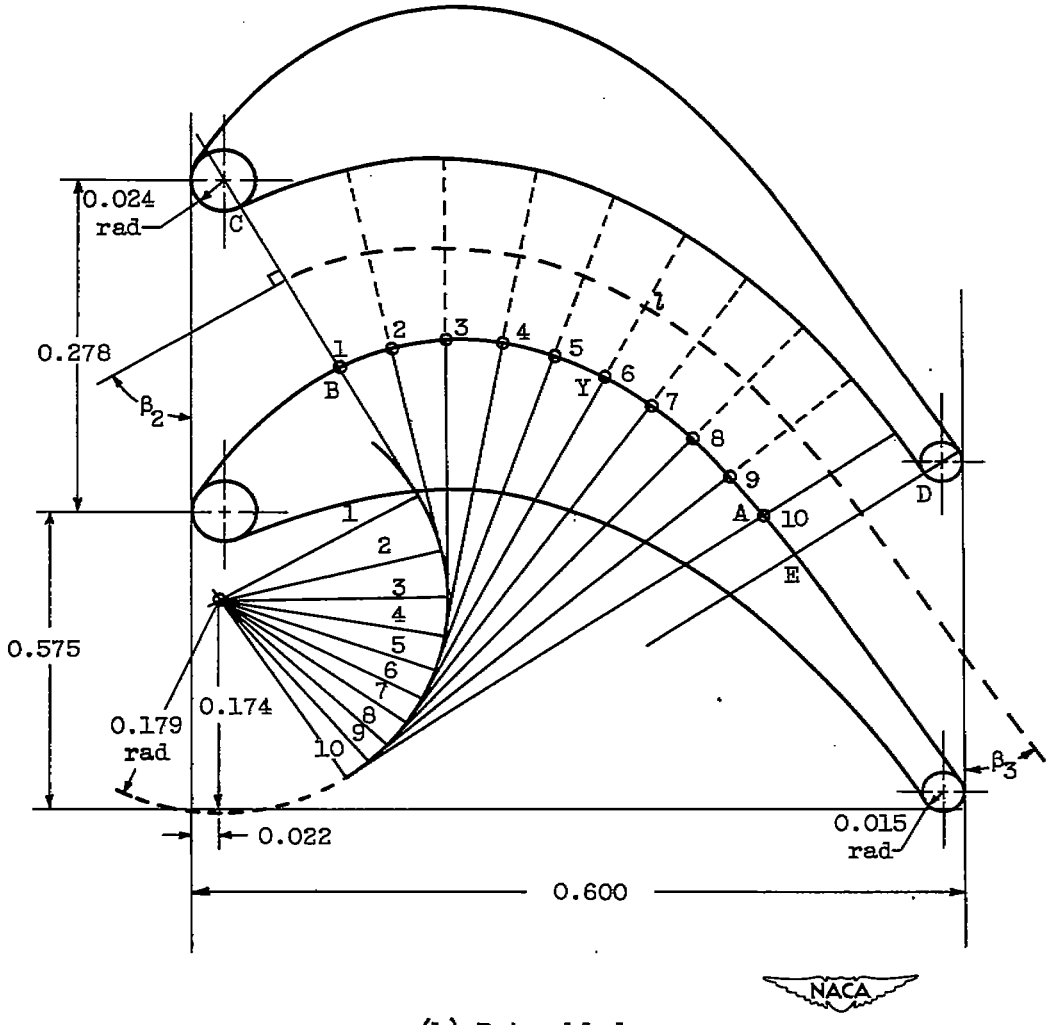

(b) Rotor blade.

Figure 3. - Concluded. Mean-section profiles of blades. (All dimensions in inches.)

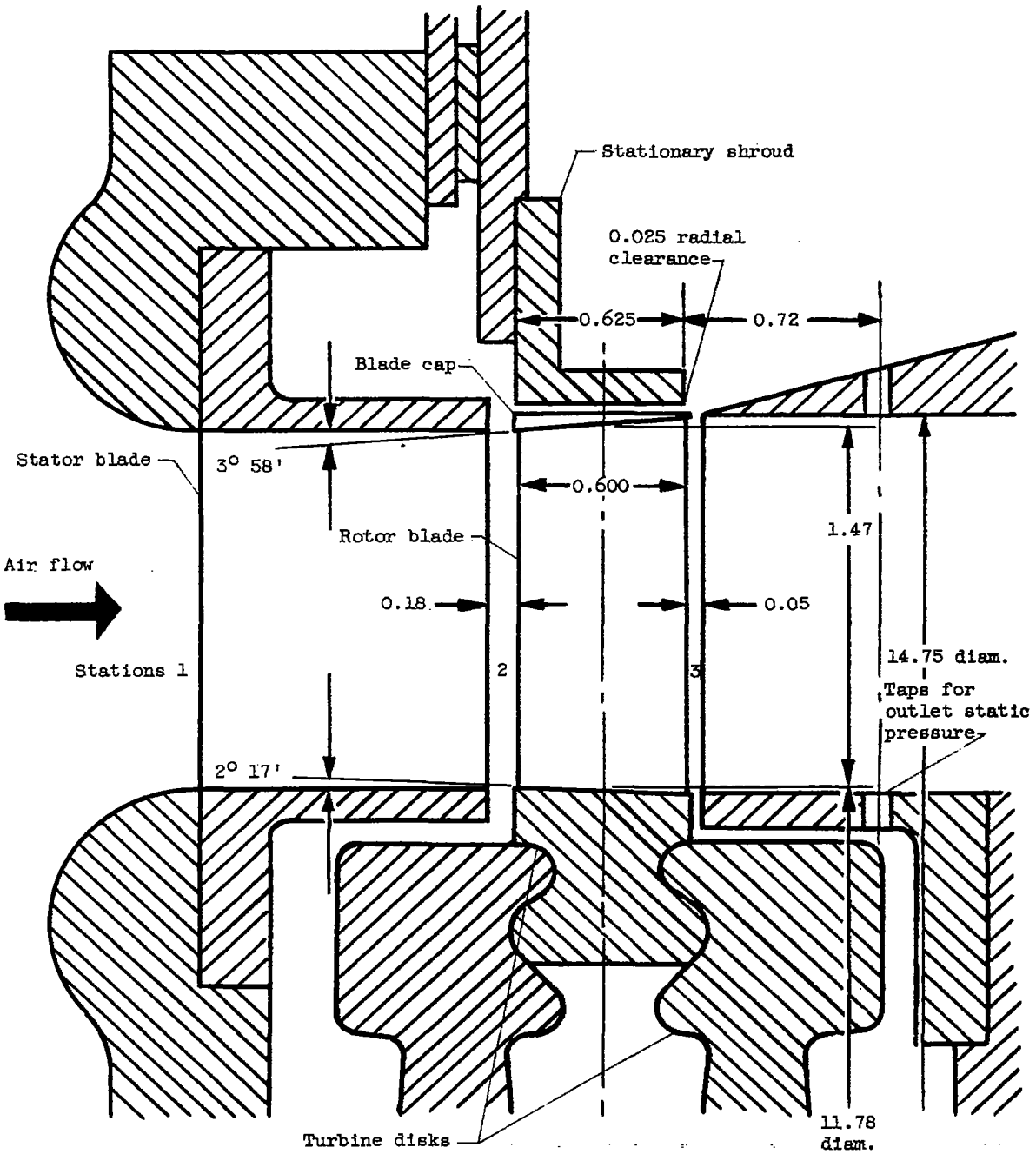

(a) Turbine-blading configuration showing turbine dimensions.

Figure 4. - Cross-sectional views of turbine blading and assembly. (All dimensions in inches.)

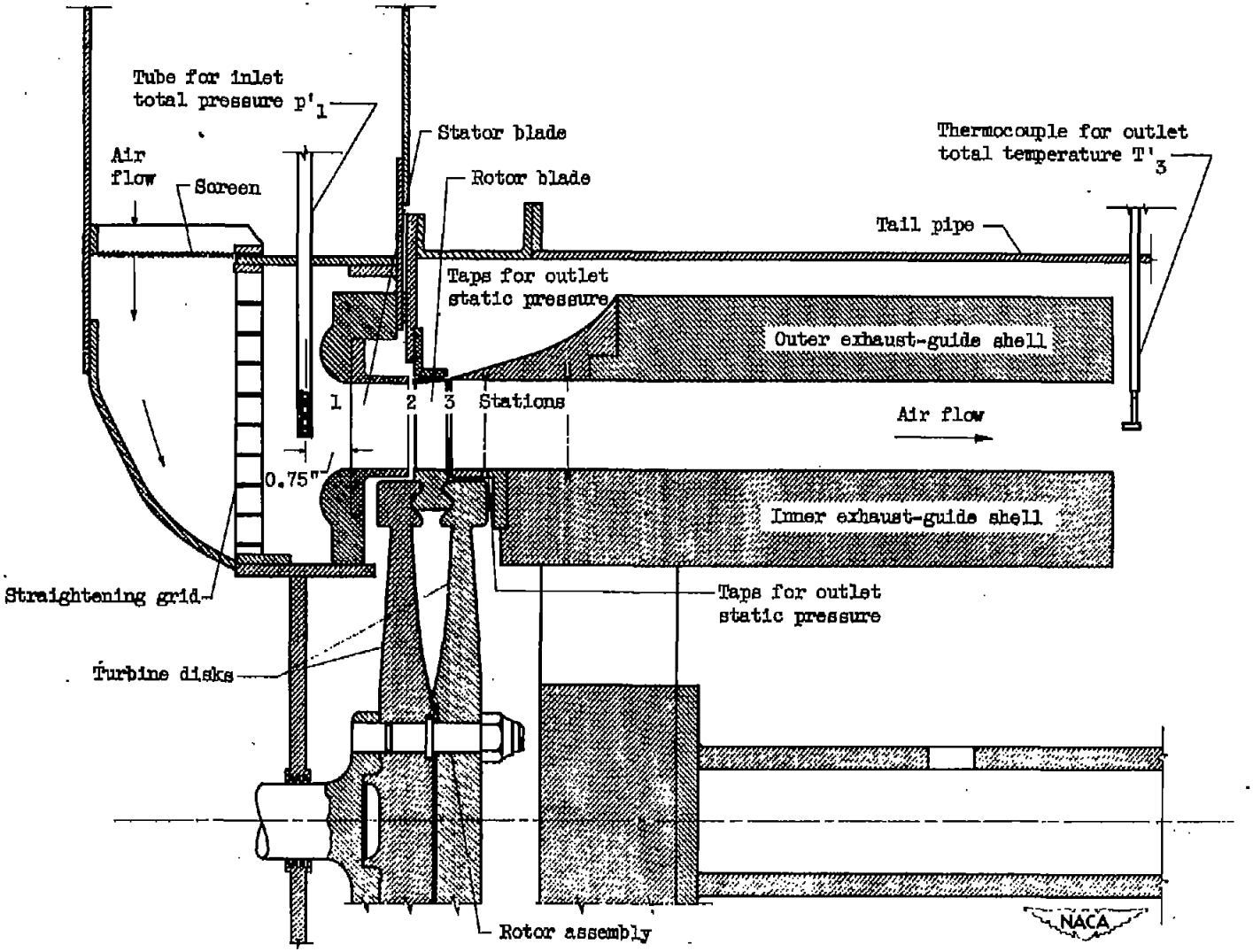

(b) Turbine assembly showing instrumentation.

Figure 4. - Concluded. Cross-sectional views of turbine blading and assembly. (All dimensions in inches.)

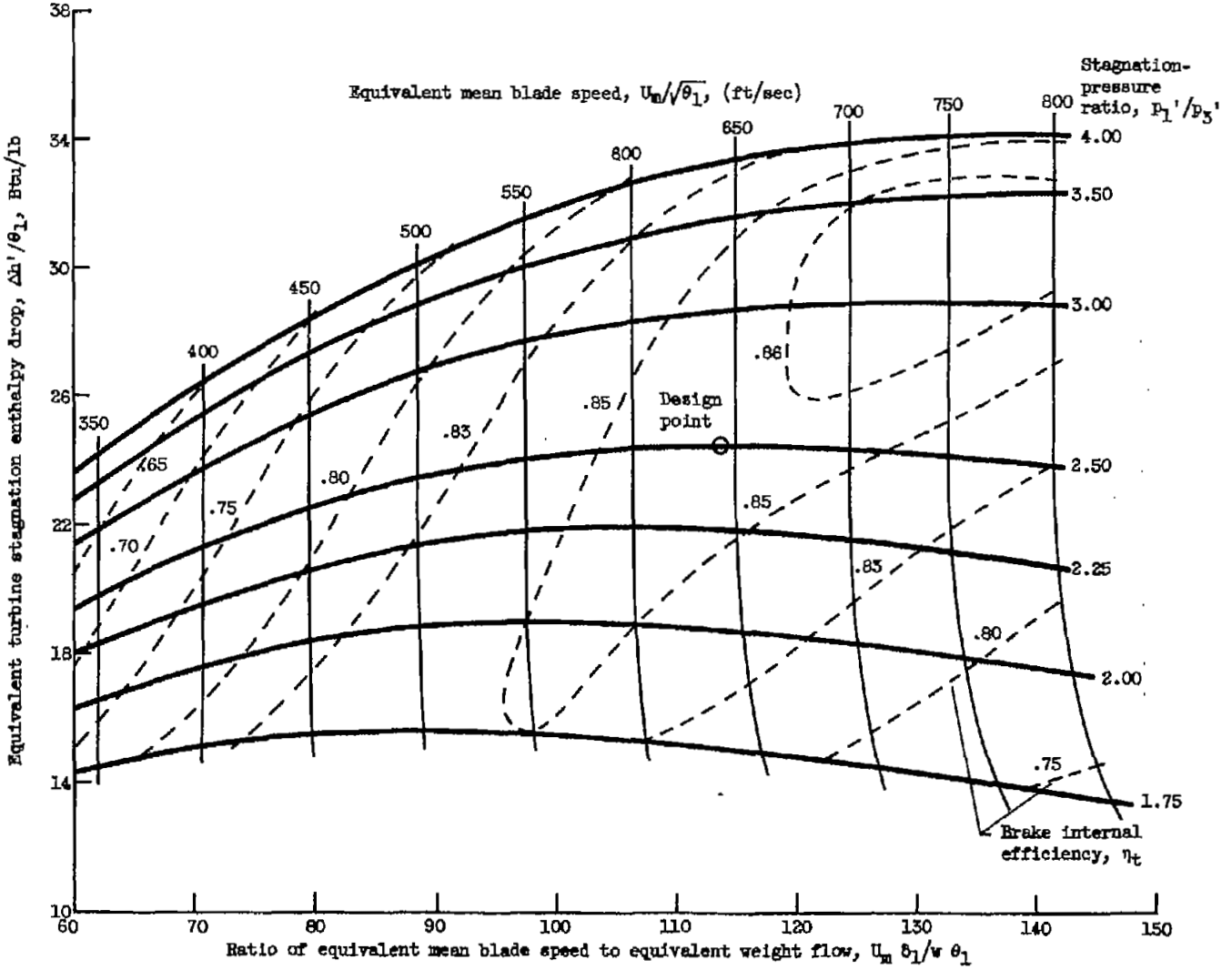

(a) Stator designed for zero rotor-incidence angles (twisted stator).

Figure 5. - Over-all performance of nontwisted rotor-blade turbine.

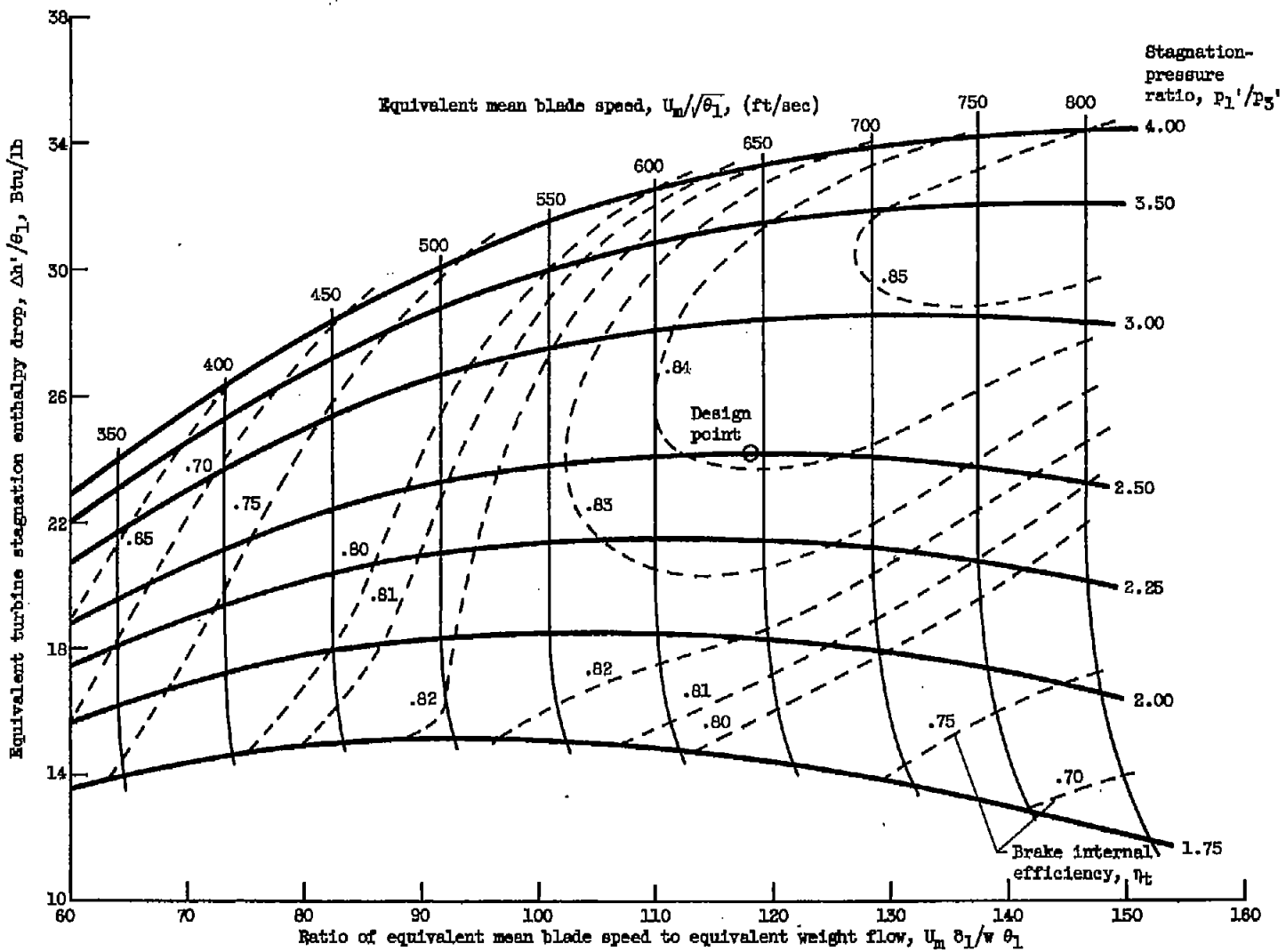

(b) Nontwisted stator.

Figure 5. - Concluded. Over-all performance of nontwisted rotor-blade turbine.

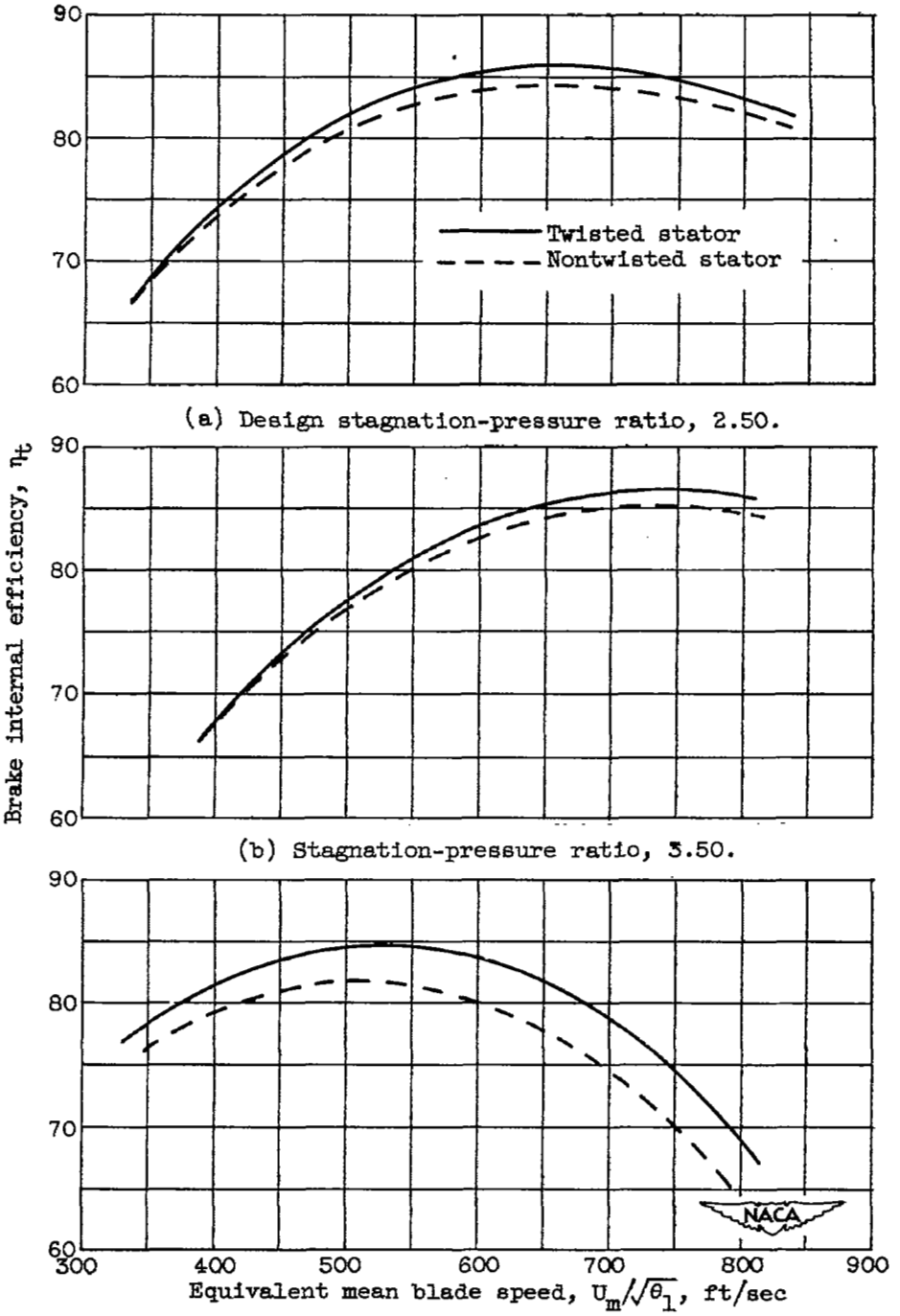

(a) Design stagnation-pressure ratio, 2.50.

(b) Stagnation-pressure ratio, 3.50.

(c) Stagnation-pressure ratio, 1.75.

Figure 6. - Comparison of brake internal efficiency for nontwisted rotor-blade turbine with twisted stator and with nontwisted stator.